Pathol. Oncol. Res. (2014) 20:755–764
DOI 10.1007/s12253-014-9758-x

REVIEW

Tricellulin Expression and its Prognostic Significance in Primary Liver Carcinomas

Áron Somorácz · Anna Korompay · Péter Törzsök · Attila Patonai · Boglárka Erdélyi-Belle · Gábor Lotz · Zsuzsa Schaff · András Kiss

Received: 28 October 2013 / Accepted: 25 February 2014 / Published online: 21 March 2014

Abstract Numerous data suggest that altered expression of tight junction proteins such as occludin and claudins plays important role in carcinogenesis. However, little is known about tricellulin, a transmembrane tight junction protein concentrated where three epithelial cells meet. We aimed to characterize tricellulin expression in normal and cirrhotic liver in comparison to primary hepatic neoplasms. Tricellulin expression of 20 control livers, 12 cirrhotic livers, 32 hepatocellular carcinomas (HCC), and 20 intrahepatic cholangiocarcinomas (iCCC) was investigated by immunohistochemistry and Western blotting. Co-localization of tricellulin with claudin-1, -4, and MRP2 was studied using double immunofluorescence. Scattered tricellulin immunopositivity was restricted to biliary pole of hepatocytes confirmed by co-localization with MRP2. Moreover, spotted-like reaction was observed between bile duct epithelial cells. In 40 % of HCCs marked tricellulin overexpression was measured regardless of tumor grades. In iCCCs, however, tricellulin expression decreased parallel with dedifferentiation. In HCCs high tricellulin expression, in iCCCs low tricellulin expression correlated with poor prognosis. Co-localization with MRP2 might substantiate that tricellulin plays role in blood-biliary barrier. Overexpressed tricellulin in a subset of HCCs correlated with unfavorable prognosis. Similar to ductal pancreatic adenocarcinoma, higher grades of iCCCs were associated with decreased tricellulin expression correlating with poor prognosis.

Keywords Tricellulin · Hepatocellular carcinoma · Cholangiocellular carcinoma · Prognosis

Á. Somorácz · A. Korompay · P. Törzsök · A. Patonai · B. Erdélyi-Belle · G. Lotz · Z. Schaff · A. Kiss (✉)
2nd Department of Pathology, Semmelweis University, Budapest, Hungary
e-mail: kiss.andras@med.semmelweis-univ.hu

Introduction

Affecting direct intercellular interactions, cell adhesion molecules play an important role in carcinogenesis and tumor progression [1]. Tight junctions (TJ) between epithelial cells are responsible for preserving the integrity of basolateral and apical membrane domains, as well as for maintaining the intercellular barrier which hinders paracellular transport. While there are numerous studies indicating that altered expression of claudins and occludin is involved in the development of malignancies [2, 3], little is known about tricellulin, a recently identified member of the tight junction protein family [4].

A novel feature of tricellulin in comparison to formerly known tight junction molecules is the cellular localization of the molecule. Namely, tricellulin mainly shows conspicuous accumulation in the cell membrane at three-cell contact sites, it can, however, also be detected in bicellular junctions [4]. Harboring two extracellular loops, four transmembrane domains, cytoplasmic N- and C-terminals, tricellulin reveals a structure similar to occludin and claudins. Moreover, its C-terminal sequence shows 32 % sequence identity with occludin [5]. Due to alternative splicing, tricellulin has different isoforms varying in size between 51 and 64 kDa. These isoforms seem to show organ specific distribution [6].

Only limited data are available on altered tricellulin expression under pathological conditions. Mutation of the tricellulin gene results in nonsyndromic hearing impairment, therefore suggesting a crucial role in cochlear and vestibular epithelial function [7]. In addition, decreased tricellulin expression was observed in tonsillar squamous cell cancers in comparison to normal mucosal epithelium [8]. In our previous studies, we characterized tricellulin expression in normal and tumorous pancreas, [9] as well as in fibrolamellar hepatocellular carcinoma, a rare subtype of hepatocellular malignancies [10].

Hepatocellular carcinoma (HCC) is the sixth most common neoplasm worldwide, showing rising incidence in the United

States and Europe. Furthermore, due to its poor prognosis, HCC ranks third in cancer related mortality [11]. Despite global increase in incidence, intrahepatic cholangiocarcinoma (iCCC), another type of primary liver cancer, is much less common [12].

Tight junctions between hepatocytes, and further, between biliary epithelial cells are of great importance in preserving the blood-biliary barrier. Claudins-1, -2 and occludin were detected in primary biliary ductules formed by hepatocytes, furthermore, claudins-3, -4, -7, -8 and -10 were also expressed in the epithelium of larger intrahepatic bile ducts [13, 14]. Moreover, it was demonstrated that claudin-1 together with occludin serve as co-receptors for hepatitis C virus [15, 16]. To complete the picture, claudin-5, as a general endothelial adhesion molecule, can be observed in hepatic sinusoidal endothelium [17]. The expression pattern of tight junction proteins changes in developing HCCs when compared with non-tumorous liver tissue. Claudin-1 expression is decreased in a subset of HCCs that is correlated with higher malignancy and poor prognosis [18]. As a contrast, overexpression of claudin-10 was correlated with worse survival and higher microvessel density, suggesting a role in tumor vascularization [19, 20]. Since claudin-5 can only be detected in sinusoidal endothelial cells of healthy liver, as well as in the endothelium of vascular structures of conventional HCCs, a surprising observation was to detect claudin-5 immunopositivity in tumor cells of fibrolamellar HCCs [10]. Possessing a distinct composition of tight junction proteins, iCCCs can be characterized by occludin, claudins-1, -2, -4 and -10 immunoreactivity [13]. In addition, claudin-18 expression was shown in 40 % of iCCCs associated with lymph node metastasis and worse overall survival [21].

In the present study, our aim was to investigate the localization and degree of tricellulin expression in healthy and cirrhotic tissue as well as in primary liver carcinomas (HCC, iCCC). We also wished to examine correlation between tricellulin expression and the level of differentiation, as well as the clinical outcome of these malignancies.

Materials and Methods

Patient Material

Eighty-four surgical liver resection specimens were investigated with approval from the Regional Ethical Committee. Thirty-two HCCs and 20 iCCCs were surgically resected. Twenty normal liver samples were obtained from peritumoral liver tissue lacking cirrhosis, inflammation, or marked fatty degeneration (3 colorectal cancer metastases, 6 HCCs and 11 iCCCs). Tissue samples from six cirrhotic livers were collected by wedge biopsy, whereas peritumoral cirrhotic tissues of six HCCs were also investigated. Excisional samples of six HCCs, six iCCCs and six normal livers were immediately snap frozen in liquid nitrogen and stored at −80 °C.

Diagnoses including tumor grading based on histopathological examination were established by expert liver pathologists (Zs. Sch., A.K. and G.L.) using routine stainings complemented with immunoreactions.

Patient data are summarized in Table 1.

Immunohistochemistry

Tricellulin immunohistochemistry was carried out on 20 control livers, 12 cirrhotic livers, 32 HCCs, and 20 iCCC samples. Three micrometer thick sections were cut from formalin-fixed, paraffin-embedded tissue blocks. After deparaffinization (xylene) and rehydration (graded ethanol), epitope retrieval was performed by enzymatic digestion using Protease 1 (Ventana, Tucson, AZ, USA) for 4 min at room temperature. Peroxidase and protein blocking, incubation with primary and secondary antibody, as well as visualization of immunoreactions were carried out applying Ventana Benchmark XT automated immunohistochemical staining system (Ventana) according to manufacturer's protocol. Slides were incubated with primary antibody for tricellulin (polyclonal rabbit, Invitrogen, Carlsbad, CA, USA) diluted 1:50 in Antibody Diluent (Ventana) for 40 min at 42 °C. Incubation with secondary anti-rabbit antibody conjugated with HRP-multimer (Ventana) was followed by application of UltraView™ Universal DAB Detection Kit (Ventana). After visualization, hematoxilin was used as counterstain.

For negative control, slides were incubated with Antibody Diluent lacking primary antibody, whereas human duodenum served as positive control.

Evaluation of Tricellulin Immunohistochemistry

For quantitative analysis of tricellulin immunoreactions, slides were scanned and digitalized by Pannoramic 250 Scanner (3D Histech, Budapest, Hungary). Fifteen randomly selected, non-overlapping fields of view were photographed from each slide at 60× virtual objective magnification. The extent of immunopositivity was measured by digital morphometry using the Leica Qwin Software (Leica, Wetzlar, Germany). The program calculated the percentage of immunopositive area (Area%) by determining the number of positive pixels in comparison to the total pixel count. Area% values of the 15 view fields were averaged.

Statistical Analysis

Sample groups were statistically compared in relation to Area% of tricellulin immunoreaction using Mann–Whitney non-parametric test according to non-Gaussian distribution. Cancer samples were divided into low-tricellulin and high-tricellulin

Table 1 Patient data

Patient group	N	M/F	Age (y)	Additional data
Control liver	20	15/5	M: 63.6 (34–79) F: 58.2 (49–78)	Concomitant lesion: CRCm (3), HCC (6), iCCC (11)
Cirrhosis	12	10/2	M: 64.5 (50–81) F: 56.5 (55–58)	Concomitant lesion: HCC (10) Etiology: HCV (2), non-viral, non-alcoholic (10)
HCC	32	26/6	M: 67.6 (47–81) F: 67.3 (46–82)	Surrounding liver: normal (6), steatosis (2), fibrosis (10), cirrhosis (14) Histological grade: I (10), II (13), III (8), mixed (1)
iCCC	20	7/13	M: 55.6 (34–79) F: 58.4 (36–78)	Surrounding liver: normal (11), steatosis (2), fibrosis (6), cirrhosis (1) Histological grade: I (5), II (9), III (6)

M/F male to female ratio, *CRCm* colorectal carcinoma metastasis, *HCC* hepatocellular carcinoma, *iCCC* intrahepatic cholangiocarcinoma, *HCV* hepatitis C virus

groups, based on median value for survival analysis performed by the Kaplan-Meier method. Further investigated parameters included patient age, tumor size and tumor grade. Correlation between tricellulin expression and other variables was examined by Spearman's rank correlation test. Cox regression analysis was applied to estimate hazard ratio of tricellulin expression regarding overall survival. Analysis was made with Statistica 7.0 software (Statsoft, Tulsa, OK, USA).

Immunofluorescence

Double immunofluorescent staining was performed on five control liver, five HCC, and five iCCC samples. Five micrometer thick sections cut from fresh frozen tissue blocks were fixed in methanol for 10 min at −20 °C. Slides were dried out at RT and were rehydrated in phosphate saline buffer (PBS, pH 7.4). Non-specific binding sites were blocked using Protein Block (Dako, Glostrup, Denmark) for 30 min at 37 °C. Slides were incubated with primary antibodies overnight at 4 °C as follows: control liver and HCC samples with either tricellulin/claudin-1 or tricellulin/MDR antibodies, iCCCs with tricellulin/claudin-4 antibody cocktail. After washing in PBS, the appropriate fluorescent secondary antibodies diluted 1:200 in PBS (Alexa Fluor 488, donkey anti-mouse; Alexa Fluor 568, goat anti-rabbit; Invitrogen) were applied according to their specificity for 30 min at RT. Sections were mounted with Fluorescent Mounting Medium (Dako) containing 4′,6-diamidino-2-phenylindole (DAPI) for nuclear staining. Immunoreactions were analyzed with Leica DM-RXA fluorescent microscope.

The main characteristics of applied antibodies are summarized in Table 2.

Protein Isolation and Western Blot Analysis

Protein was extracted from snap frozen tissue blocks of six control liver, six HCC, and six iCCC samples. Fifty milligrams of each sample was pulverized in liquid nitrogen followed by homogenization in lysis buffer containing 20 mM TRIS pH7.5, 150 mM NaCl, 2 mM EDTA, 1 % TritonX-100 and protease inhibitor cocktail (Sigma Aldrich, St Louis, MO, USA). Protein concentration was determined according to Bredford protein assay. Appropriate volume of lysates containing 30 μg of protein was submitted to polyacrylamide gel electrophoresis on 10 % SDS-polyacrylamide gel applying 200 V for 35 min. Separated protein samples were blotted on nitrocellulose membrane for 75 min at 100 V and 4 °C. Blotting was controlled by Ponceau S red staining. Non-specific protein binding sites were saturated with 5 % non-fat dry milk (Sigma) for 30 min at RT. Membranes were incubated with tricellulin (1:500) and GAPDH (mouse monoclonal; AbDSerotec, Kidlington, UK; 1:5000) antibodies diluted in TRIS-buffered saline (TBS) containing 1 % non-fat dry milk overnight at 4 °C. After washing with TBS-Tween (0.1 % Tween 20) solution, HRP-conjugated secondary antibodies (anti-rabbit and anti-mouse; Dako) diluted 1:2000 in TBS were applied for 2 h at RT. Finally, membranes were incubated with enhanced chemiluminescence solution (BioRad, Hercules, CA, USA) for visualization. Immunoreactions were analyzed using Kodak Gel Documentation System (Kodak, Rochester, NY, USA).

Results

Tricellulin Expression in Normal Liver Tissue

Normal liver showed heterogeneous tricellulin immunostaining. Dominantly, faint reaction was detected, however in a subset of samples strong immunopositivity was observed. The reaction was detected both on hepatocytes and biliary epithelial cells. Dot-like accumulations in a linear pattern were seen in the internal area of hepatocyte plates (Fig. 1a). Double

Table 2 Antibodies applied in the study. The C-terminal consensus sequence was detected by anti-tricellulin antibody

Antigen	Type	Clone	Application	Dilution	Manufacturer
Claudin-1 (H)	mouse monoclonal	2H10D10	IF	1:100	Invitrogen
Claudin-4 (H)	mouse monoclonal	3E2C1	IF	1:100	Zymed
MRP2 (H)	mouse monoclonal	M2III-6	IF	1:50	Abcam
Tricellulin (H)	rabbit polyclonal	–	IHC, IF, WB	1:50, 1:50, 1:500	Invitrogen

H human, *MRP*2 multidrug resistance-related protein 2, *IF* immunofluorescence, *IHC* immunohistochemistry, *WB* western blot

immunofluorescent reaction showing co-localization with claudin-1 (Fig. 2a, b, c), and MRP2 protein (Fig. 2d, e, f), confirmed the localization of tricellulin between hepatocytes along primary biliary ductules. Moreover, immunofluorescence emphasized conspicuous dot-like accumulations at three cell contact sites which were inserted in a linear membrane staining. On the other hand, spotted-like pattern of immunoreaction was observed between biliary epithelial cells at their apical pole of bile ducts in portal tracts, as well as in larger sized bile ducts (Fig. 1b). By Western blot analysis, week bands were detected at ~60 kDa (Fig. 3).

Tricellulin Expression in Cirrhotic Liver

In cirrhotic tissue, tricellulin immunohistochemistry showed similar pattern to control liver samples. Linear and dot-like reaction was seen in the parenchyma of nodules, whereas spotty pattern was localized apically in the biliary epithelium of proliferating bile ducts.

Tricellulin Expression in HCCs

The extent and intensity of tricellulin immunoreaction varied over a wide range in HCCs samples. On one hand, some HCCs showed no positivity, on the other hand, marked overexpression of tricellulin was detected in a subset of tumors. In pseudoglandular structures of well or moderately differentiated carcinomas, similar expression pattern was detected as seen in biliary epithelium. Namely, membranous staining was observed at the apical pole of tumor cells with dot-like enhancement at cell-contact sites (Fig. 4a). Linear pattern with spotty accumulations was characteristic in disorganized tumorous trabeculi and cell nests (Fig. 4b). Strong positivity was even observed in some poorly differentiated HCCs (Fig. 4c). Double immunofluorescent reaction revealed co-localization of tricellulin and claudin-1 in HCCs (Fig. 2g, h, i). However, disorganized expression of both tight junction components was observed, resulting in non-overlapping reactions. In addition, besides membranous staining, nuclear positivity was also demonstrated in a minor subset (1–2 %) of tumor cells in six HCC samples (Fig. 5). Five of these HCCs showed only very weak membranous staining.

A ~60 kDa protein was detected in each HCC investigated by Western blot analysis, however, a larger product at 80 kDa was also seen in 4/6 samples (Fig. 3).

Tricellulin Expression in iCCCs

Both the strength and extent of tricellulin immunoreaction showed an obvious decrease related to the dedifferentiation of iCCCs. Higher tumor grade was clearly associated with decreased tricellulin protein expression. The pattern of immunreaction in glandular structures of well differentiated tumors was identical to that observed in normal bile ducts (Fig. 4g). In non-glandular carcinomas with tumor cells lacking polarity, tricellulin immunostaining was either weak or absent (Fig. 4i). Tricellulin was found co-localized with claudin-4 in iCCCs based on double immunofluorescence

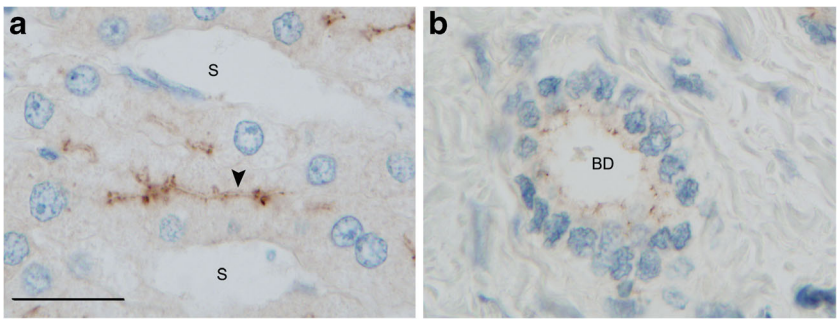

Fig. 1 Tricellulin expression in normal liver. Tricellulin was demonstrated between hepatocytes along primary biliary ductules (*arrowhead*) (**a**). Immunopositivity localized to the apical segment of biliary epithelial cells. Tricellulin was found in larger bile ducts as well (**b**). S: sinusoid; BD: bile duct. Scalebar 25 μm

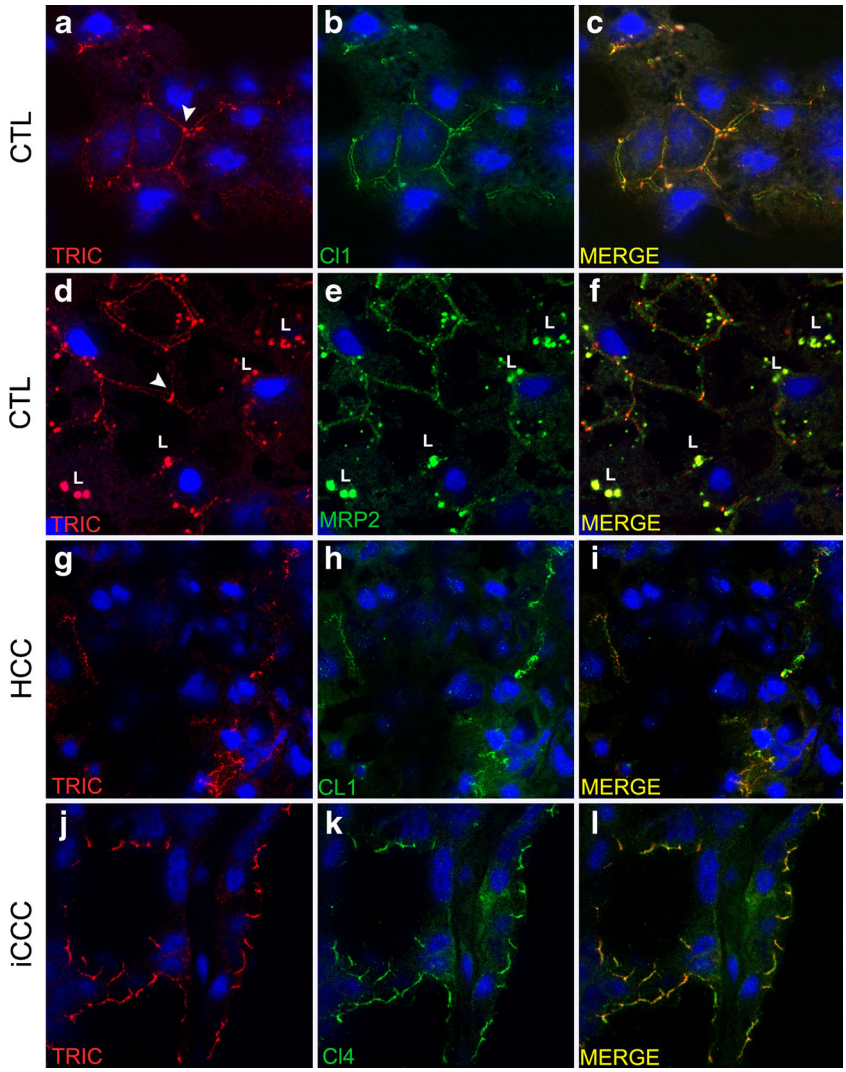

Fig. 2 Co-localization of tricellulin with claudin-1, claudin-4, and MRP2. In normal liver, tricellulin was concentrated mainly at three cell contact sites (*arrowhead* in **a** and **d**), however, linear pattern according to bicellular junctions was seen as well (**a**, **d**). Co-localization with MRP2 was demonstrated in normal liver (**d**–**f**), and with claudin-1 in both normal liver (**a**–**c**) and HCCs (**g**–**i**) G shows HCC with moderate expression of tricellulin. Lipofuscin labeled 'L' showed strong aspecific autofluorescence (**d**–**f**). Tricellulin co-localized with claudin-4 in iCCCs (J-L) CTL: control liver; Cl1: claudin-1; Cl4: claudin-4; MRP2: multidrug resistance protein 2; TRIC: tricellulin

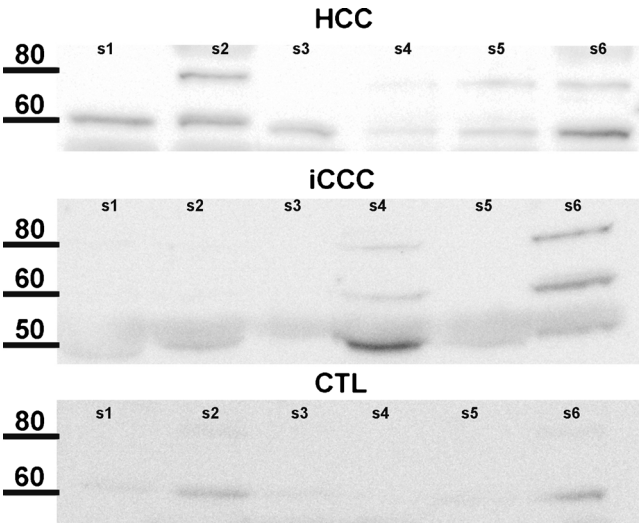

Fig. 3 Western blot analysis of tricellulin in HCC, iCCC, and control liver samples

(Fig. 2j–l). Western blot analysis detected tricellulin in well differentiated cholangiocarcinomas (2/6). Similarly to HCCs, both the ~60 kDa and ~80 kDa products were demonstrated. Moreover, a specific band at 50 kDa was also observed in one sample (Fig. 3).

Morphometric Analysis of Tricellulin Immunohistochemistry

Comparing normal samples with cirrhotic livers and HCCs, no significant difference was calculated based on tricellulin expression rate measured by digital morphometry (Fig. 6). Interestingly, however, 40 % of HCCs showed more than two times higher overexpression compared to the median value of normal liver samples. Moreover, tricellulin expression was increased in 5/6 HCCs as compared with their non-cirrhotic, non-tumorous adjacent liver tissue. No correlation was found between tricellulin expression and tumor grading, tumor size and age.

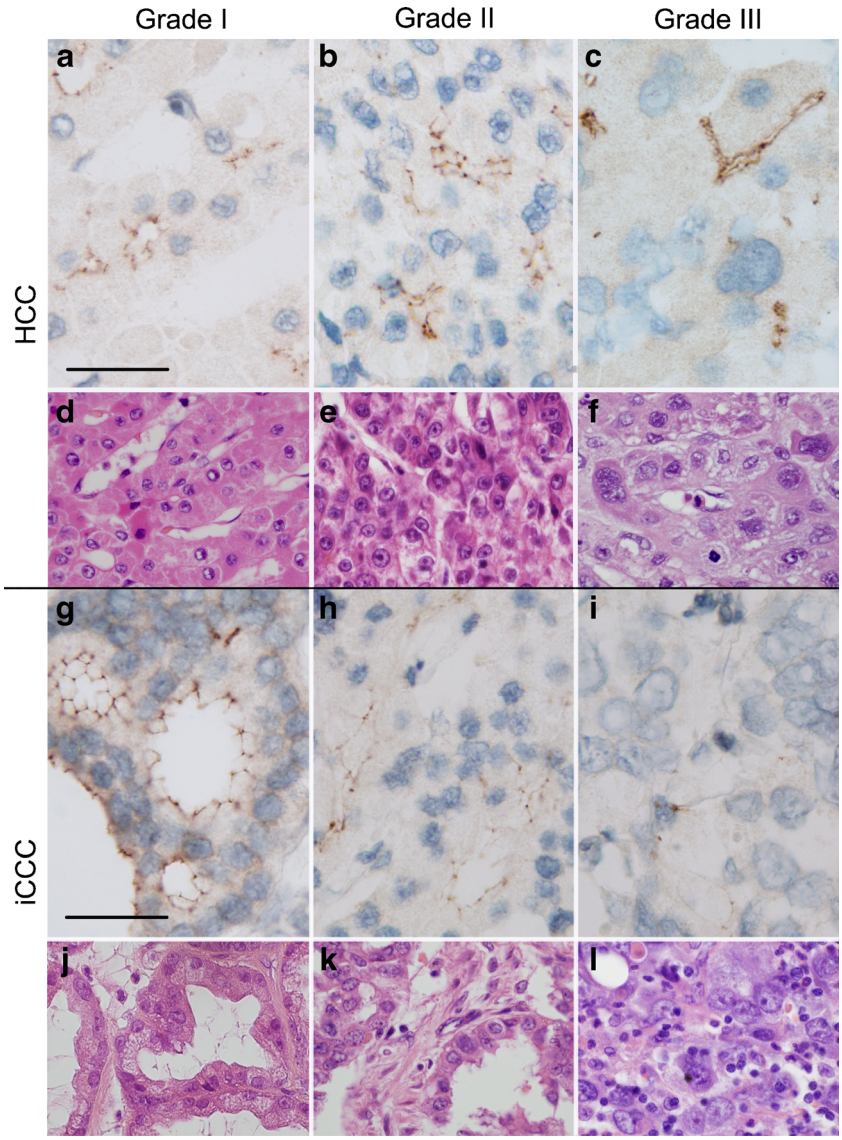

Fig. 4 Tricellulin expression in HCCs and iCCCs. Pseudoglandular structures of well differentiated HCCs revealed tricellulin immunostaining pattern similar to that found in bile ducts (**a**). Linear and dot-like reaction was observed in irregular trabeculi of HCCs (**b**). Immunopositivity was even detected in some poorly differentiated HCCs (**c**). Tricellulin immunopositivity was strong and diffuse in well differentiated (**g**), partially preserved in moderately differentiated (**h**), and weak or absent in poorly differentiated (**i**) cholangiocarcinomas. Corresponding areas of **h & e** stainings of HCCs (**d**, **e**, **f**) and iCCCs (**j**, **k**, **l**). Scalebar 25 μm

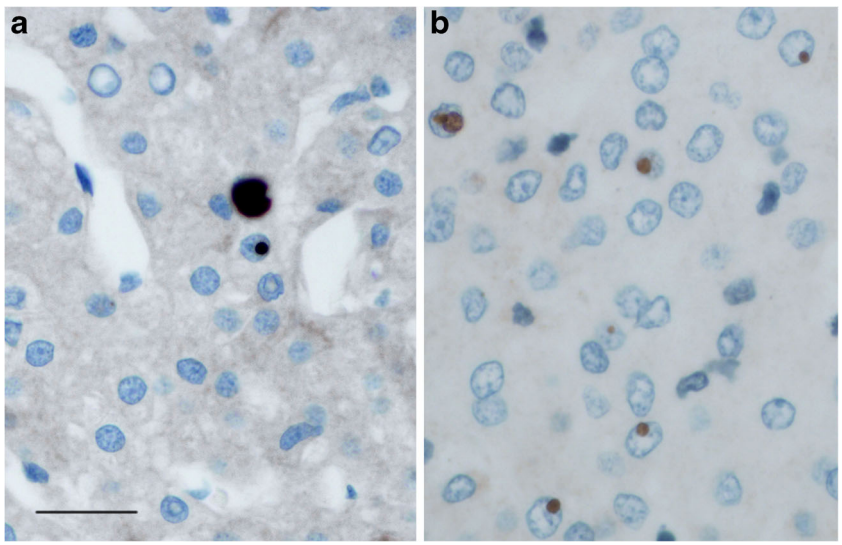

Fig. 5 Nuclear tricellulin positivity in HCCs. Nuclear positivity was detected in 6 HCCs in 1–2 % of tumor cells. There were areas revealing nuclear tricellulin staining reactions with weak (**a**), or without (**b**) membrane staining. Scalebar 25 μm

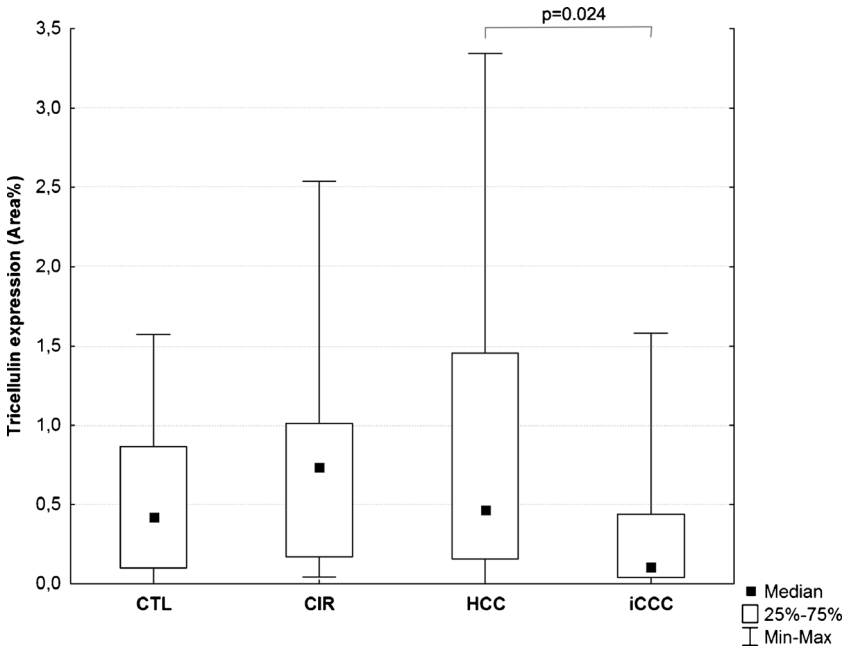

Fig. 6 Morphometric analysis of tricellulin immunohistochemistry in control livers, cirrhotic livers, HCCs, and iCCCs. Each sample group was characterized by large deviations resulting in non-significant differences. However, the highest values were measured in well- and moderately differentiated HCCs. (Mann–Whitney *U*-test) Cir: cirrhosis; CTL: control liver

On the other hand, iCCCs revealed significantly decreased tricellulin expression in comparison to HCCs (Fig. 6). Unlike in HCCs, marked decrease of tricellulin expression was observed in iCCCs parallel with dedifferentiation that resulted in a significant difference ($p<0.05$) between glandule forming grade I cancers and non-glandular grade III tumors with solid growing pattern (Fig. 7).

Survival Analysis of Liver Cancers

HCC and iCCC samples were divided into "tricellulin-low" and "tricellulin-high" groups based on being above or below the median value of tricellulin Area% measured by digital morphometry. In addition, tumor grading, tumor size and age were also used for grouping variables. Spearman's rank correlation test proved that the investigated grouping variables were independent factors.

There was no correlation between tumor grading, tumor size as well as age, and overall survival calculated by Kaplan-Meier analysis. However, high tricellulin expression of HCC was associated with shorter survival time ($p<0.05$). Cox regression analysis estimated a hazard ratio of 3.12 for "tricellulin-high" tumors (CI: 1.35–7.2; $p<0.01$).

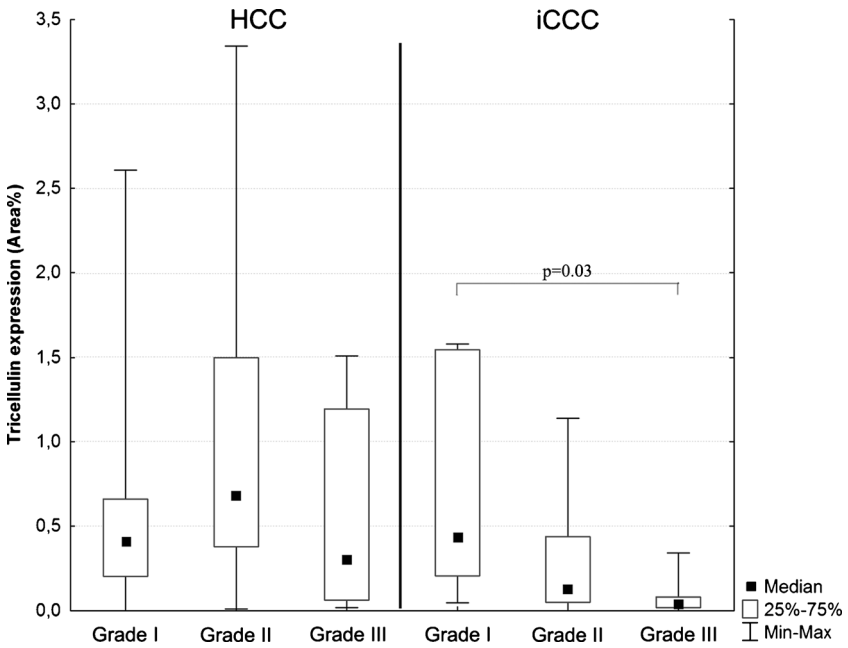

Fig. 7 Morphometric analysis of tricellulin immunohistochemistry in different grades of HCCs and iCCCs. While different grades of HCCs did not reveal significant expressional differences, marked and significant decrease of tricellulin expression was observed in dedifferentiated grade III iCCCs in comparison to well differentiated grade I cancers. (Mann–Whitney *U*-test)

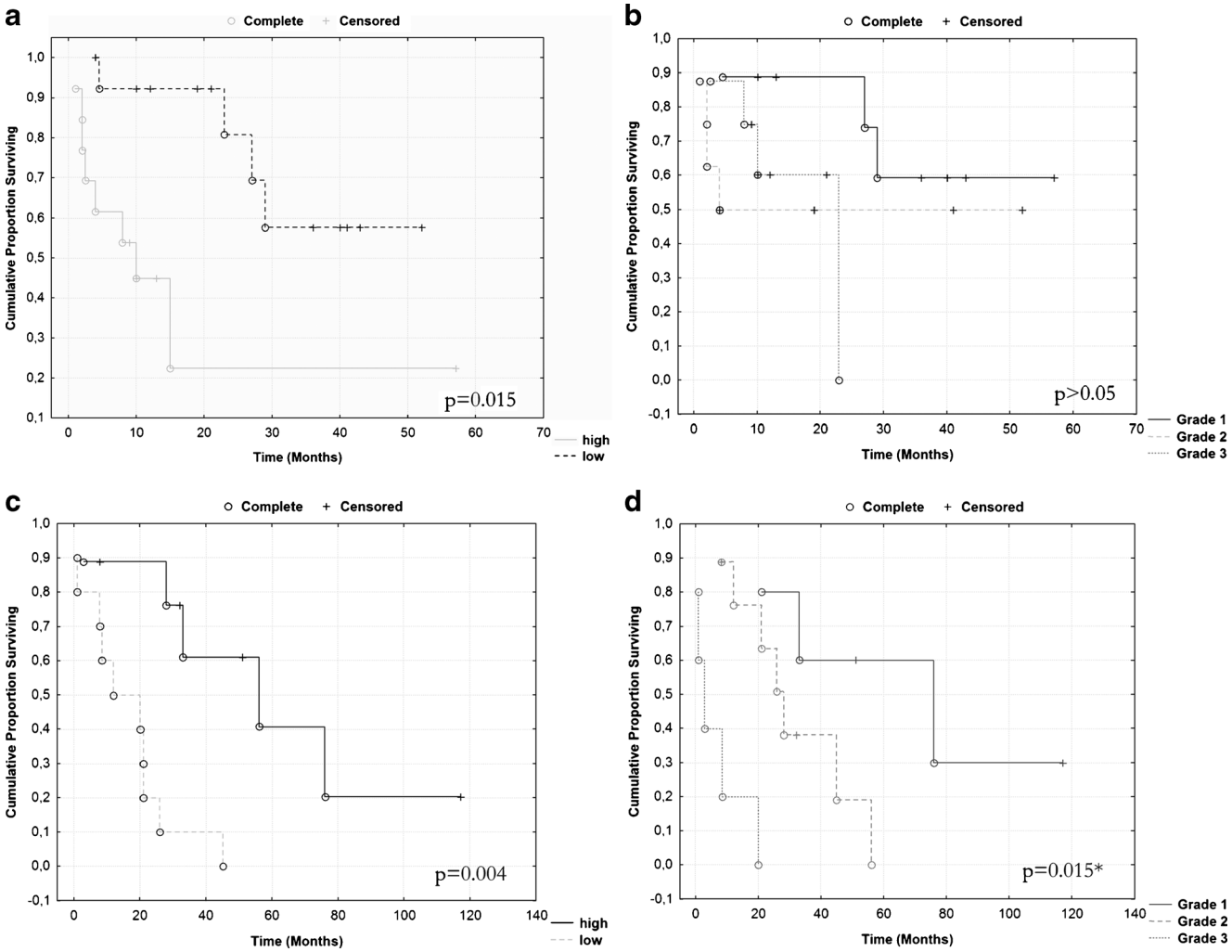

Fig. 8 Survival analysis of HCCs and iCCCs. High tricellulin expression was associated with poor prognosis in HCCs (**a**), whereas tumor grading showed no correlation with survival (**b**). On the other hand, high tricellulin expression characteristic for well differentiated tumors was correlated with better overall survival in iCCCs (**c**), which was reflected in tumor grading as well (**d**). (Kaplan-Meier analysis)

In contrast, "tricellulin-high" iCCCs had better prognosis in comparison to "tricellulin-low" tumors ($p<0.05$). As tricellulin expression varied parallel with iCCC grading based on the level of differentiation, groups were also identified by tumor grades according to overall survival ($p<0.05$) (Fig. 8).

Discussion

Tight junctions of hepatocytes and biliary epithelial cells establish a polarization that results in the maintenance of an apical (biliary) and basolateral membrane domain, and which is essential in the excretion and transport of bile. Transmembrane tight junction proteins such as occludin and claudins close paracellular gaps and create a blood-biliary barrier that is necessary for proper liver function [22]. Our study revealed tricellulin expression along biliary tree from canaliculi to large bile ducts. Moreover, it showed a marked accumulation at three cell contact sites and it was present in bicellular junctions as well, both on hepatocytes and biliary epithelium. An interesting observation in our study was the heterogeneous expression and considerably wide range of strength and rate of positivity on both normal and tumorous hepatocytes, varying from virtually zero to strong and diffuse immunopositivity. Specificity of the reaction was also ensured by the positivity of larger bile ducts as internal controls, which were positive in every normal and peritumoral liver sample.

Beyond structural function in the blood-biliary barrier, recent studies revealed that liver tight junction proteins as claudin-1 and occludin, which were seen by us co-localized with tricellulin, could also act as co-receptors for HCV and facilitate viral entry into hepatocytes. In vitro experiments indicated that claudin-1 and occludin have an important role in the late phase of entry [15, 16], moreover, claudins-6 and −9 could also potentially possess similar function [23, 24]. Based on the analog molecular structure, tricellulin might possibly also be involved in this process, which hypothesis merits further investigation.

Several studies demonstrated that both overexpression and downregulation of tight junction proteins can occur during carcinogenesis and these changes are not necessarily continuous with progression. In HCCs, claudin-1 and −10 protein expression was related to clinicopathological features of tumors. While a decrease in claudin-1 level was determined in poorly differentiated HCCs [18], overexpression of claudin-10 was detected in about 40 % of liver cancers and was shown to predict poor survival [19, 20] In our present study, HCCs—similarly to control liver samples—showed a wide range of tricellulin expression rate finally resulting in no significant difference between the two groups. Five HCCs out of the six HCC-adjacent non-cirrhotic liver tissue pairs showed increased expression when compared with the surrounding liver. In view of this, hepatocarcinogenesis might be associated with upregulation of tricellulin expression in certain cases. On the other side, tricellulin immunoreactivity showed no correlation with tumor grading, tumor size, etiology factor and age.

Nuclear presence of a tight junction protein might represent different biological processing of the protein, which may be related to genetic aberration or a posttranslational modification. For example, nuclear localization of claudin-1 correlated with PKA-induced phosphorylation in melanoma cells [25]. Further, tight junction proteins might have function in signal transduction [26]. In our present study, nuclear tricellulin positivity was demonstrated in 19 % of HCCs. Moreover, nuclear staining was associated with weak membranous reaction in the majority of this sample subset, which presumes disturbed intracellular trafficking of tricellulin. The molecular background of altered subcellular localization, however, requires further investigation.

We recently detected decreased tricellulin expression associated with dedifferentiation of pancreatic ductal carcinoma [9], which phenomenon was observed in this study regarding iCCCs as well. Loss of differentiation in adenocarcinomas is manifested in disrupted glandule formation that can appear even as single-cell infiltration. This process is thought to be correlated with disintegration of tight junctions based both on decreased expression or altered distribution of adhesion molecules. Thus, both overexpression and downregulation of tight junction proteins can be detected in carcinogenesis [27, 28]. However, both processes might result in declining intercellular contact and paracellular permeability [29]. This duality occurs in iCCCs as well, since claudin-4 was found to be overexpressed independent of tumor grade as compared with normal biliary epithelium [14].

The impact of tight junction proteins on biological behavior of tumors is diverse. One protein could be associated with either attenuated or higher malignancy depending on cancer type [30, 31]. On the other hand, certain tight junction proteins could act as tumorsuppressor, while others as tumor promoter in the same tumor type [18, 20]. In HCCs, similarly to claudin-10, high tricellulin expression rate was correlated with shorter overall survival and proved to be an independent risk factor. On the contrary, in iCCCs—composing another type of primary liver cancers with distinct origin and a "classic adenocarcinoma" histological pattern—the preserved tricellulin expression was associated with significantly better clinical outcome in comparison to tumors with low tricellulin expression. This correlation was associated with dedifferentiation/grading of iCCC cells.

In conclusion, we identified tricellulin as a component of hepatic tight junctions, both between human hepatocytes and biliary epithelial cells, suggesting role in the blood-bile barrier. Independent of grading, HCCs reveal heterogeneous tricellulin expression, whereas an obvious, significant decline of tricellulin expression was found parallel with dedifferentiation in iCCCs similarly to the finding in ductal pancreatic adenocarcinoma. High tricellulin expression in HCCs, however, correlated with poor overall survival, while decreased expression in iCCCs was associated with poor prognosis.

Acknowledgments This work was supported by grants from the Hungarian Scientific Research Found (OTKA)# K101435.

Disclosure Statement The authors have no financial or personal conflicts of interest to disclose.

References

1. Zigler M, Dobroff AS, Bar-Eli M (2010) Cell adhesion: implication in tumor progression. Minerva Med 101:149–162
2. Turksen K, Troy TC (2011) Junctions gone bad: claudins and loss of the barrier in cancer. Biochim Biophys Acta 1816:73–79
3. Martin TA, Mason MD, Jiang WG (2011) Tight junctions in cancer metastasis. Front Biosci 16:898–936
4. Ikenouchi J, Furuse M, Furuse K et al (2005) Tricellulin constitutes a novel barrier at tricellular contacts of epithelial cells. J Cell Biol 171: 939–945
5. Chiba H, Osanai M, Murata M et al (2008) Transmembrane proteins of tight junctions. Biochim Biophys Acta 1778:588–600
6. Riazuddin S, Ahmed ZM, Fanning AS et al (2006) Tricellulin is a tight-junction protein necessary for hearing. Am J Hum Genet 79: 1040–1051
7. Chishti MS, Bhatti A, Tamim S et al (2008) Splice-site mutations in the TRIC gene underlie autosomal recessive nonsyndromic hearing impairment in Pakistani families. J Hum Genet 53:101–105
8. Kondoh A, Takano K, Kojima T et al (2011) Altered expression of claudin-1, claudin-7, and tricellulin regardless of human papilloma virus infection in human tonsillar squamous cell carcinoma. Acta Otolaryngol 131:861–868
9. Korompay A, Borka K, Lotz G et al (2012) Tricellulin expression in normal and neoplastic human pancreas. Histopathology 60(6B):E76–E78
10. Patonai A, Erdelyi-Belle B, Korompay A et al (2011) Claudins and tricellulin in fibrolamellar hepatocellular carcinoma. Virchows Arch 458:679–688
11. Parkin DM, Bray F, Ferlay J et al (2005) Global cancer statistics, 2002. CA Cancer J Clin 55:74–108

12. Hammill CW, Wong LL (2008) Intrahepatic cholangiocarcinoma: a malignancy of increasing importance. J Am Coll Surg 207:594–603
13. Nemeth Z, Szasz AM, Tatrai P et al (2009) Claudin-1, -2, -3, -4, -7, -8, and -10 protein expression in biliary tract cancers. J Histochem Cytochem 57:113–121
14. Lodi C, Szabo E, Holczbauer A et al (2006) Claudin-4 differentiates biliary tract cancers from hepatocellular carcinomas. Mod Pathol 19: 460–469
15. Liu S, Yang W, Shen L et al (2009) Tight junction proteins claudin-1 and occludin control hepatitis C virus entry and are downregulated during infection to prevent superinfection. J Virol 83:2011–2014
16. Evans MJ, von Hahn T, Tscherne DM et al (2007) Claudin-1 is a hepatitis C virus co-receptor required for a late step in entry. Nature 446:801–805
17. Sakaguchi T, Suzuki S, Higashi H et al (2008) Expression of tight junction protein claudin-5 in tumor vessels and sinusoidal endothelium in patients with hepatocellular carcinoma. J Surg Res 147:123–131
18. Higashi Y, Suzuki S, Sakaguchi T et al (2007) Loss of claudin-1 expression correlates with malignancy of hepatocellular carcinoma. J Surg Res 139:68–76
19. Huang GW, Ding X, Chen SL et al (2011) Expression of claudin 10 protein in hepatocellular carcinoma: impact on survival. J Cancer Res Clin Oncol 137:1213–1218
20. Cheung ST, Leung KL, Ip YC et al (2005) Claudin-10 expression level is associated with recurrence of primary hepatocellular carcinoma. Clin Cancer Res 11:551–556
21. Shinozaki A, Shibahara J, Noda N et al (2011) Claudin-18 in biliary neoplasms. Its significance in the classification of intrahepatic cholangiocarcinoma. Virchows Arch 459:73–80
22. Kojima T, Yamamoto T, Murata M et al (2003) Regulation of the blood-biliary barrier: interaction between gap and tight junctions in hepatocytes. Med Electron Microsc 36:157–164
23. Meertens L, Bertaux C, Cukierman L et al (2008) The tight junction proteins claudin-1, -6, and -9 are entry cofactors for hepatitis C virus. J Virol 82:3555–3560
24. Zheng A, Yuan F, Li Y et al (2007) Claudin-6 and claudin-9 function as additional coreceptors for hepatitis C virus. J Virol 81:12465–12471
25. French AD, Fiori JL, Camilli TC et al (2009) PKC and PKA phosphorylation affect the subcellular localization of claudin-1 in melanoma cells. Int J Med Sci 6:93–101
26. Terry S, Nie M, Matter K et al (2010) Rho signaling and tight junction functions. Physiology (Bethesda) 25:16–26
27. Gonzalez-Mariscal L, Lechuga S, Garay E (2007) Role of tight junctions in cell proliferation and cancer. Prog Histochem Cytochem 42:1–57
28. Lal-Nag M, Morin PJ (2009) The claudins. Genome Biol 10:235
29. de Oliveira SS, de Oliveira IM, De Souza W et al (2005) Claudins upregulation in human colorectal cancer. FEBS Lett 579:6179–6185
30. Yoshida T, Kinugasa T, Akagi Y et al (2011) Decreased expression of claudin-1 in rectal cancer: a factor for recurrence and poor prognosis. Anticancer Res 31:2517–2525
31. Shin HI, Kim BH, Chang HS et al (2011) Expression of claudin-1 and -7 in clear cell renal cell carcinoma and its clinical significance. Korean J Urol 52:317–322